High strain-rate tensile testing and viscoplastic parameter identification using microscopic high-speed photography

Kajberg, J.; Sundin, K. G.; Melin, L. G.; Ståhle, P.

Published in:
International Journal of Plasticity

DOI:
10.1016/S0749-6419(03)00041-X

2004

Document Version:
Peer reviewed version (aka post-print)

PERGAMON

International Journal of Plasticity 20 (2004) 561–575

INTERNATIONAL JOURNAL OF Plasticity

www.elsevier.com/locate/ijplas

High strain-rate tensile testing and viscoplastic parameter identification using microscopic high-speed photography

J. Kajberg[a], K.G. Sundin[a,*], L.G. Melin[b,1], P. Ståhle[a,2]

[a] *Division of Solid Mechanics, Luleå University of Technology, SE-97187 Luleå, Sweden*
[b] *Division of Experimental Mechanics, Luleå University of Technology, SE-97187 Luleå, Sweden*

Received in revised form 4 February 2003

Abstract

A combined experimental/numerical method for determination of constitutive parameters in high strain-rate material models is presented. Impact loading, using moderate projectile velocities in combination with small specimens (sub mm) facilitate tensional strain rates in the order of 10^4–10^5 s^{-1}. Loading force is measured from one-dimensional wave propagation in a rod using strain gauges and deformation is monitored with a high-speed camera equipped with a microscope lens. A sequence of digital photographs is taken during the impact loading and the plastic deformation history of the specimen is quantified from the photographic record. Estimation of material parameters is performed through so called inverse modelling in which results from repeated FE-simulations are compared with experimental results and a best choice of constitutive parameters is extracted through an iterative optimisation procedure using the simplex method. Results are presented from a preliminary tension test of a mild steel (A533B) at a strain rate well over 10^4 s^{-1}. The sensitivity of the evaluated material parameters to errors in measured quantities is studied. The method, especially the optical technique for measurement of deformation will be further developed.

Keywords: B. Constitutive behaviour; B. Viscoplastic material; C. Impact testing; C. Optimization; High-speed photography

* Corresponding author. Tel.: +46-920-491284; fax: +46-920-491047.
E-mail address: karl-gustav.sundin@mt.luth.se (K.G. Sundin).
[1] Now at FOI, Swedish Defence Research Agency, SE-17290 Stockholm, Sweden.
[2] Now at Malmö University Materials Science, SE-20506 Malmö, Sweden.

0749-6419/03/$ - see front matter
doi:10.1016/S0749-6419(03)00041-X

1. Introduction

A technical material is usually characterised mechanically by its stress–strain curve measured under static conditions in a standard tensile test. In such tests the strain rate in the specimen is small, usually of the order of 10^{-2} s^{-1}. However, in many technical applications and processes, material is deformed under conditions that imply strain rates many orders of magnitude higher than in the standard tensile test. Examples of such processes are plastic forming and cutting. Also in unintended situations like collisions and impacts material is deformed at rates that can be very high.

A technically important situation that also involves large strains and high strain rates is the growth of a crack. A complex state of multi-axial stress and strain prevails in the vicinity of the crack tip. In metals the local deformation is generally plastic and the strains are large. Even if the global loading is quasi-static, very high plastic strain-rates can be at hand close to the crack tip due to the small length scale. In the case of a propagating crack it is obvious that material is strained from zero to fracture as the crack tip passes and this process necessarily involves high strain-rates. It has been suggested that micro-cracking ahead of the main crack, leads to an irregular crack front containing small, more or less isolated regions of material, bridging the two main crack surfaces (Hogland, et al., 1972). These regions or ligaments will experience very high strain rates when they are torn off as the surfaces separate during crack propagation. The energy consumed by the plastic processes at the crack tip will influence the propagation speed and the eventual arrest of the crack tip. The constitutive description of the material, especially in terms of the rate-dependence, plays an important role in the modelling of this problem (Freund and Hutchinson, 1985; Brickstad, 1983; Lo, 1983; Nilsson, et al., 1998).

Complex, often rate dependent phenomena on micro-structural, molecular or atomic level are active during plastic deformation of a solid material. For metals the physical explanation of the rate dependence in the constitutive relations is based on the fact that dislocation movement is subject to rate dependent drag forces. In for example (Barlat et al., 2002), models for dislocation behaviour and its impact on mechanical properties are presented and discussed. Unfortunately it is not yet possible to accurately predict macroscopic material behaviour under high-rate conditions from dislocation theory and therefore empirical models must be used. Such models must be calibrated in carefully designed experiments, through which parameters in the models can be identified. For mild steel elastic-viscoplastic models are generally used for the mechanical description of high rate deformation processes. Such models have been suggested by for example Perzyna (1963), Johnson and Cook (1983, 1985) and Zerilli and Armstrong (1987). For reviews of the area see for example Lemaitre and Chaboche (1990) and Meyers (1994). Viscoplastic constitutive models for high strain-rate deformation of some metals are also discussed in more recent papers, for example Liang and Khan (1999), Khan and Liang (1999) and Nemat-Nasser and Kapoor (2001). Other materials, for example polymers and wood, also exhibit rate dependent mechanical behaviour although the underlying physical processes obviously are different from those in metals. High-rate

experiments are necessary in order to establish numerical models for transient events involving such materials. Recent reports of such experiments are for example Khan and Lopez-Pamies (2002) for a soft polymer and Widehammar (2002) for spruce wood. As long as efficient models including material parameters are not well known among engineers, it is probably safe to state that the demand for experimental work regarding high-rate constitutive modelling of materials will remain high.

Classical experiments for determination of constitutive parameters generally utilise specimens designed to give a homogeneous state of stress, strain and strain rate in a volume of the tested materiel. Practical requirements regarding mechanical attachment and strain measurement tend to demand this volume to be fairly large and high strain rates are therefore hard to achieve in conventional testing machines.

Methods like Split Hopkinson Pressure Bar (or Kolsky Bar), Rotating flywheel and Drop tower are used for high strain-rate testing. These methods generally also utilise a state of homogeneous stress and strain in the specimen for direct evaluation of material parameters. Relatively large specimens are therefore needed also in these cases and high strain rates therefore require high impact velocities. In compression strain rates of 10^5 s^{-1} are reached in extreme experiments (Pope and Field, 1984; Gorham et al., 1992). Special versions of the split Hopkinson pressure bar have been developed for tensile and shear testing and strain rates of 10^3 s^{-1} are typical in these applications. Comprehensive reviews of experimental methods can be found in textbooks and review papers (see for example Meyers, 1994; Blazynski, 1987; Lindholm, 1971; Field et al., 1994; Gray, 2000).

In this paper a combined experimental and numerical method that does not require a homogeneous state of stress and strain is suggested and a pilot study is performed. Specimens can be made small if a nonhomogeneous state is allowed and thus high strain rates can be achieved at rather low impact velocities. A small specimen with a non-homogenous state of stress and strain has been used also by Gilat and Cheng (2000, 2002) to reach high strain rates. The method presented here uses microscopic high-speed photography to record information regarding the deforming geometry. Due to its non-contacting nature the suggested method is expected to be suitable also for high temperature testing. In this first study, the general principle, some preliminary test results and a sensitivity analysis are presented. One material and one viscoplastic constitutive model are studied.

2. Experiments

A small specimen is loaded in tension by a transient force so that it is rapidly stretched to fracture. The specimen has the shape of a small ligament of material formed by two deep, adjacent notches in a rod of rectangular (5×3 mm^2) cross section as shown in Fig. 1. The length, L, of the ligament is only a fraction of a millimetre (0.4 mm) in order to obtain a high strain rate when tearing the ligament axially. In this preliminary experiment the width, W, of the ligament, that is the distance between the two adjacent notches, was chosen small (0.24 mm) in comparison with the thickness of the ligament, which is 3 mm as determined by the cross

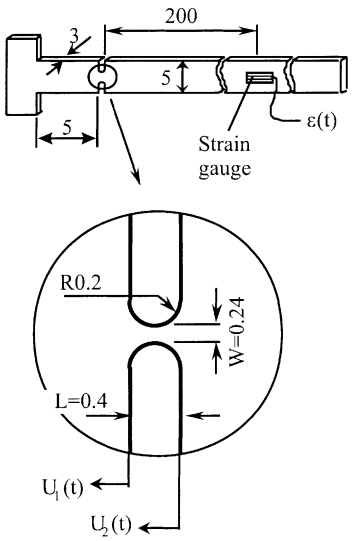

Fig. 1. The geometry of the specimen rod and the ligament (specimen). All numbers are in mm.

sectional dimension of the rod. With this geometry, a state of approximately plane strain will prevail through most of the thickness of the ligament. The rod in which the ligament is machined is 500 mm long with a T-shaped head at one end for application of the axial load. At a distance of 5 mm from the head the notches forming the ligament were machined out using the method of electric wire discharge. This method allows narrow notches to be formed, using a thin wire, and thus a short specimen can be obtained facilitating high strain rates. A quenched and tempered A533B grade B class 1 steel with yield stress 345 MPa was chosen for this investigation. This steel is used in the nuclear power industry and good understanding of its mechanical behaviour, including the mechanics of propagating cracks, is of interest.

A diagram of the experimental set-up is presented in Fig. 2. The arrangement shown in this figure is designed for tensile loading of the specimen rod but compressive loading can easily be achieved in a similar experiment. The head of the specimen rod is attached to one end of a loading rod with the aid of a yoke (not shown in figure). The loading rod is made of steel, it is 1.5 m long and has a diameter of 25 mm. Both rods are supported horisontally by plastic bearings with low friction and the specimen rod is arranged along the side of the loading rod. The loading rod is impacted axially by a projectile with a flat end-surface and the generated elastic wave propagates along the rod. As the wave reflects, the T-shaped head of the specimen rod is loaded towards the left in Fig. 2. The ligament is rapidly torn to fracture in the axial direction with an extension rate that is of the same order as the velocity of the impacting projectile. As the material in the ligament is stretched to fracture the tensile force generates an elastic wave in the specimen rod. This tensile wave is measured by a pair of strain gauges, (KYOWA KFG-5-120-C1-11L1M2R) positioned 0.2 m from the ligament (see Fig. 1). The amplified strain signal is recorded by a transient recorder and transferred to a computer. The

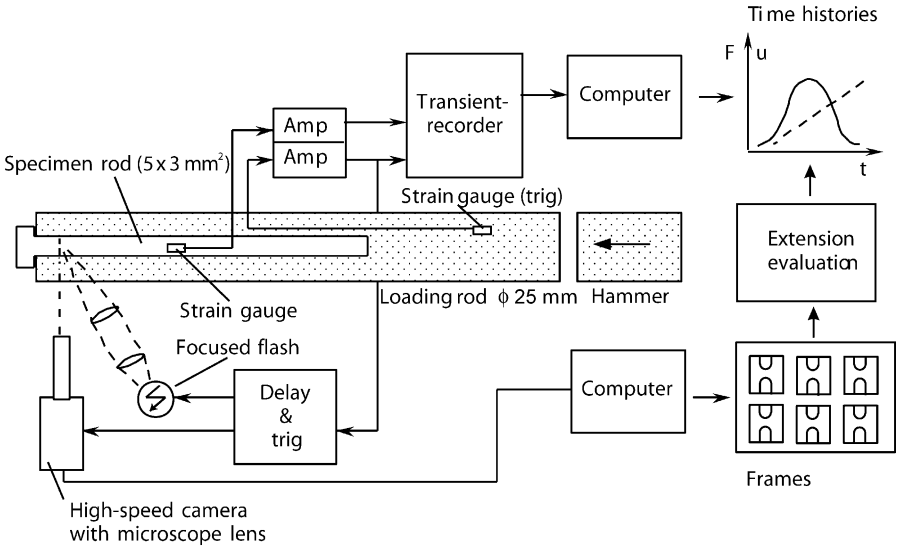

Fig. 2. Experimental set-up.

recorded strain history, multiplied with Young's modulus and cross-sectional area of the specimen rod, is taken as the force history, $F^{\exp}(t)$, in the ligament during the rapid tearing to fracture (see Fig. 3).

It should be noted here that the duration of the force history shown in Fig. 3 is about 20 μs implying a wave length in the specimen rod of about 0.1 m. The tensional fracture of the specimen is therefore over before the wave has reached the far end of the 0.5 m long specimen rod. Also the positioning of the strain gauge in the middle of the specimen rod facilitates recording of the reflected wave from the free end without overlapping. From comparison of the primary and the reflected

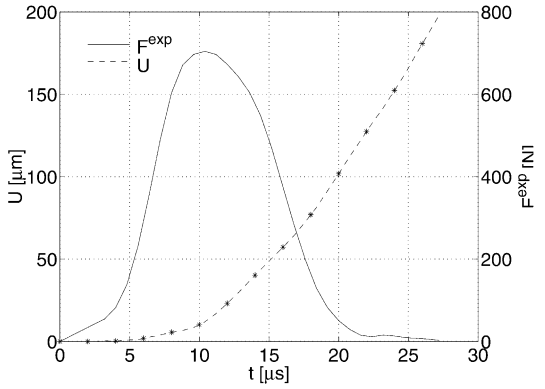

Fig. 3. Measured time histories for the force $F^{\exp}(t)$ (solid line) and the extension $U(t)$ (stars) evaluated from high-speed photographs.

wave it is possible to verify that disturbances from for example bending are negligible.

A high-speed camera of image-converter type (ULTRANAC FS 501) with a CCD-unit is used to record the tearing process in 15 frames with an exposure time of 0.4 μs and an interval between frames of 2 μs. The camera is equipped with a long distance microscope lens, which makes it possible to study an area of approximately 1.5×1.5 mm^2 with a stand-off distance of about 0.1 m. A high-voltage electrical discharge from a capacitor is used to illuminate the target. The light from the discharge is focused onto a diffuser just in front of the target area with the aid of a standard Köhler illumination system. The duration of the discharge is sufficiently long to cover the entire tearing event but the light intensity is somewhat reduced towards the end of the experiment and therefore the exposure time is increased a little for the later frames.

A strain gauge on the loading rod is used as triggering source. After a time delay, which is adapted to the travel time for the wave in the loading rod, the flash and the high-speed camera are fired. Also the transient recorder that registers the force history is triggered.

An example of the photographic record of an experiment is shown in Fig. 4. The sequence covers the entire event from unloaded to completely broken ligament and the progressive plastic deformation manifests itself through the visible extension of the ligament and also through the out-of-plane deformation of the plastically strained material at the illuminated face causing a darker appearance of the ligament. The difference in appearance of the two sides of the ligament that can be observed in Fig. 4 is caused by the oblique incidence of the illumination.

The extension of the ligament was quantified from the digital high-speed photographs and from the recorded force history in two steps. First, the displacement of

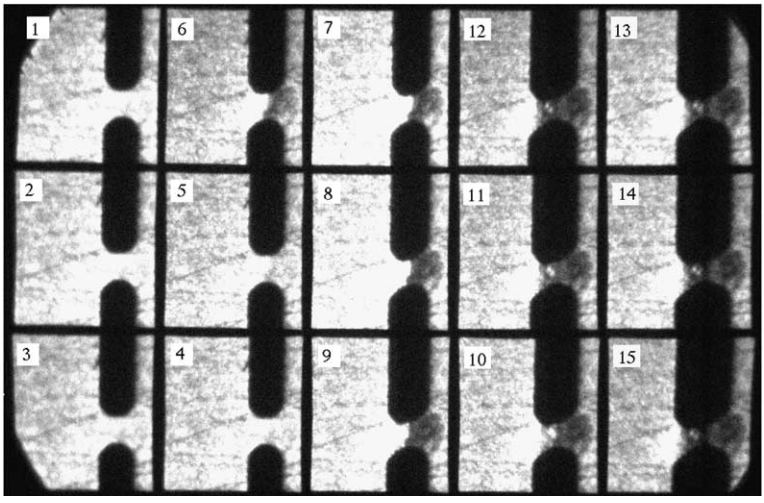

Fig. 4. High-speed photographs of deforming ligament. Frame interval 2 μs. Each frame covers approximately 1.5×1.5 mm^2.

the two sides of the ligament, $U_1(t)$ and $U_2(t)$ (Fig. 1), were measured by tracking the position (pixel-number in the digital picture) of the contrast change associated with the edges of the groove in the high-speed frames. This measure was taken at a position approximately 0.8 mm from the centre of the ligament. As a second step, the displacement of the right end of the ligament, $U_2(t)$, was controlled using one-dimensional wave theory. This control was made because the lower contrast on this side of the ligament introduced some uncertainty in the pixel counting. The alternative displacement, $U_2'(t)$, was calculated from the recorded strain history in the specimen rod according to $U_2'(t) = c\int_0^t \varepsilon(\tau)\mathrm{d}\tau$, where c is the one-dimensional wave speed and $\varepsilon(t)$ is the measured tensile strain history with the time delay associated with the wave propagation in the specimen rod cancelled. Displacement $U_2'(t)$ calculated in this way agrees with the somewhat uncertain evaluation of displacement from the contrast change at the right edge in the photographs. That is $U_2'(t) \approx U_2(t)$ and $U(t) = U_1(t)\text{-}U_2(t)$ is therefore taken as the correct measure of the extension of the ligament. In Fig. 3, $U(t)$ is presented at the times when high-speed photographs are taken and the time history is approximated by a spline function through these points.

3. Estimation of material parameters

3.1. Inverse modelling

A high strain-rate event such as the described experiment is usually modelled with an elastic–viscoplastic material model. Such a model comprises a linear elastic part for low stress levels and a viscoplastic part for high stress levels. Hooke's law is used to describe the material behaviour at low stress levels and a rate dependent model is used for the high stress levels. The rate dependent model chosen here is the one suggested by Perzyna (1963), in which the plastic strain rates are given by

$$\dot{\varepsilon}_{ij}^{p} = \begin{cases} \frac{3}{2}\gamma\left(\frac{\sigma_e}{\sigma_0} - 1\right)^n \frac{S_{ij}}{\sigma_e}, & \sigma_e > \sigma_0 \\ 0, & \sigma_e \leqslant \sigma_0 \end{cases} \tag{1}$$

where σ_e is the effective stress according to von Mises, σ_0 is the yield stress and S_{ij} is the deviatoric stress. The model also contains two unknown parameters, namely the strain rate sensitivity, γ, and the over stress exponent, n. In this study these parameters are estimated through so called inverse modelling which is an iterative process using repeated FE-calculations with varied parameters and comparison between numerical and experimental results. The method used for the inverse modelling is the subspace-searching simplex method, Subplex (Rowan, 1990). This method is designed to iterate towards minimum of an objective function through so-called direct searching. That is, the value of the objective function is calculated for stepwise varied values of parameters in an iterative sequence in order to find minima. The objective function chosen in this case consists of the sum of the squared residuals defined as

$$\Phi = \sum_{i=1}^{N} \left(f_i^{\exp}(u) - f_i^{FE}(u) \right)^2, \quad N = 31, \tag{2}$$

$$f^{\exp} = \frac{F^{\exp}}{\sigma_0 A}, \quad f^{FE} = \frac{F^{FE}}{\sigma_0 A}, \quad u = \frac{U}{L} \tag{3}$$

where A is the cross sectional area of the centre of the ligament (0.72 mm^2), $f_i^{\exp}(u)$ and $f_i^{FE}(u)$ are experimentally and numerically obtained force values at 31 equally spaced extension values in curves as those shown in Fig. 5. The curves are derived from the force and extension histories corresponding to the experiment and the FE-calculation. The numerically calculated curve in Fig. 5 is the result obtained with the optimal set of parameters. In order to ensure that a determined minimum is a global one several different pairs of starting values for the parameters γ and n have been used in the optimisation sequence.

3.2. FE-model

An updated Lagrangian method for large deformation elastic–viscoplastic materials (ABACUS/Standard 5.8) was used for the FE-calculations. The constitutive behaviour of the material is described by Hooke's law for the elastic part and by Eq. (1) for the plastic part. Material parameters are; Young's modulus $E = 210$ GPa, Poisson's ratio $\nu = 0.3$ and yield stress $\sigma_0 = 345$ MPa. As the thickness of the specimen rod (3 mm) is much greater than the other dimensions of the ligament ($L = 0.4$ mm, $W = 0.24$ mm) a state of plain strain is assumed through the thickness of the modelled ligament.

A so called boundary layer solution is applied for limitation of the FE-model. Consider a large, linearly elastic, plane body with a ligament of width W on the

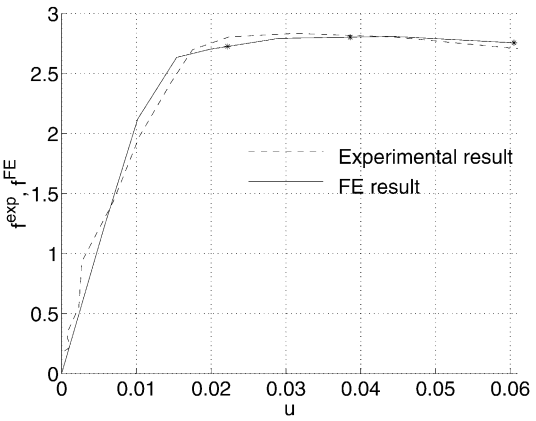

Fig. 5. Normalised force versus normalised extension. The stars indicate times when strain fields are evaluated from the FE-simulation.

symmetry-plane $y=0$ as shown in Fig. 6. It is loaded remotely by a force in the y-direction and it can be shown (Muskhelishvili, 1953; Nilsson et al., 1998) that the displacement in the y-direction for points on a semicircle of radius R, is approximately independent of the angle Θ for large values of the ratio $2R/W$. As the plastic zone in the centre of the model is small this solution can be applied and the loading of the model is therefore defined by a prescribed displacement history $U(t)/2$ in the axial direction of all the nodes along the perimeter R. In the FE-calculations $R=2.5$ mm is used, which is the distance from the centre of the ligament to the outer edge of the specimen rod. Thus $2R/W \approx 20$ which is large enough to motivate the approximative boundary layer solution. $U(t)$ is the measured extension at approximately $R/3$ as described by the dashed curve in Fig. 3. Using the extension history measured at radius $R/3$ as input at radius R in the FE-calculations implies that elastic deformations within the semicircular region are neglected in comparison to the large plastic deformations in the ligament. The force F^{FE} used in the objective

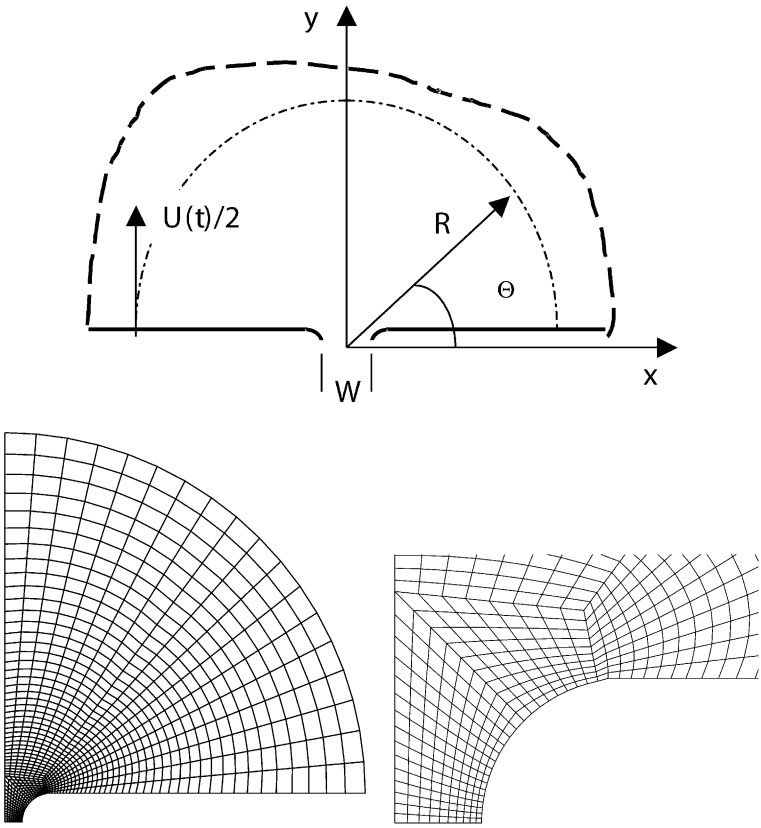

Fig. 6. The modelled semicircular region, the entire mesh and a magnification of the region with the highest element density.

function Φ [Eqs. (2) and (3)] is the resulting force on the circular boundary due to the applied controlled displacement.

A quasi-static approach is adopted in the FE-calculations. This is motivated by the fact that transit times for mechanical waves through the studied structure are much shorter than characteristic times for the load. Therefore equilibrium of forces is well developed and inertia forces are negligible.

3.3. Sensitivity analysis

Important for the usefulness of the method is how uncertainty in the measurement affects the values of the estimated parameters, γ and n in the constitutive model. In order to obtain a rough picture of this sensitivity, systematic relative uncertainties were introduced in the experimental force and extension histories. Uncertainty levels of $\pm 2\%$, $\pm 5\%$ for both force and extension were chosen and a new set of optimal material parameters were determined for every combination of uncertainty levels. These new sets of material parameters are compared with the initial ones and the sensitivity of evaluated parameters to systematic errors in measured data can thereby be estimated.

4. Result and discussion

The experimental results from the force and extension measurements are shown in Fig. 3. As mentioned above the experimental results are the basis for the FE-calculation and inverse modelling. However, the use of the experimental data needs some comments.

The basis for the force measurement is one-dimensional wave propagation in the specimen rod assuming a negligible influence from the complex stress state close to the ligament. Dispersion can have an influence on the propagating wave but it is believed to be negligible because the pulse appears to have a smooth shape. Also an electromagnetic disturbance from the flash system was observed early in the force history, but as it appeared to be repeatable it was subtracted from the force signal. As the specimen rod was freely supported with very low friction, reflected waves were observed and their similarity to the primary wave verified that disturbances from bending, dispersion and electromagnetic transient fields are of little importance.

The usefulness of the measured strain history in the specimen rod as a representation of the force history in the ligament depends on the magnitude of the inertia force that is associated with the acceleration of the specimen (ligament). A very rough and overestimated measure of the acceleration is calculated by differentiating the displacement history, $U_1(t)$ (splined), twice. The result is a very noisy function representing acceleration of the left side of the ligament which is observed to be always less than 3×10^6 m/s^2 during the experiment. The mass of the ligament is approximately 2×10^{-6} kg and it can therefore be concluded that the inertia force on the ligament is less than 6 N at all times during the experiment. This highly

overestimated value is very small compared to the measured force and therefore static conditions are assumed in the FE-analysis for simplicity in this preliminary study.

A problem with a high-speed camera of the image converter type is that relatively large aberrations might be introduced in the imaging. Different parts of the image might therefore render the object at slightly different scales. Such problems can be avoided if the camera is calibrated. At this preliminary stage these aberrations are not taken into consideration. Such optical errors are however believed to be small and without significant influence on measured ligament extension.

The complete force and extension histories are not included in the inverse analysis which is obvious from a comparison of Figs. 3 and 5. Data for later times, $t > 12$ μs, are excluded in order to avoid influence from unwanted phenomena associated with late times in the evaluation of material parameters. The data used in the inverse analysis are assumed to cover the viscoplastic hardening but not the necking at high strain levels which takes place in the ligament for later times. With this restriction in the use of force and extension histories the deformations in the FE-model do not cause so large distortions of the elements that time consuming remeshing is necessary. Another phenomenon which is avoided by the truncation of the data is the formation of microcracks and voids which is beyond the validity of the chosen constitutive model.

The yield stress, σ_0, in Eq. (1) is in general a function of plastic strain, $\sigma_0(\varepsilon_p)$, thus describing a strain-dependent yield stress. In the present calculations, a constant value of the yield stress was used in accordance with the original suggestion in Perzyna (1963). This rough model neglects static strain hardening and is chosen in this pilot study for its simplicity. The value of the yield stress was obtained from a static tension test.

The inverse analysis resulted in the parameter values, $\gamma = 25{,}000\ \mathrm{s}^{-1}$ and $n = 7$. The Subplex algorithm converged to the same values for all tested combinations of

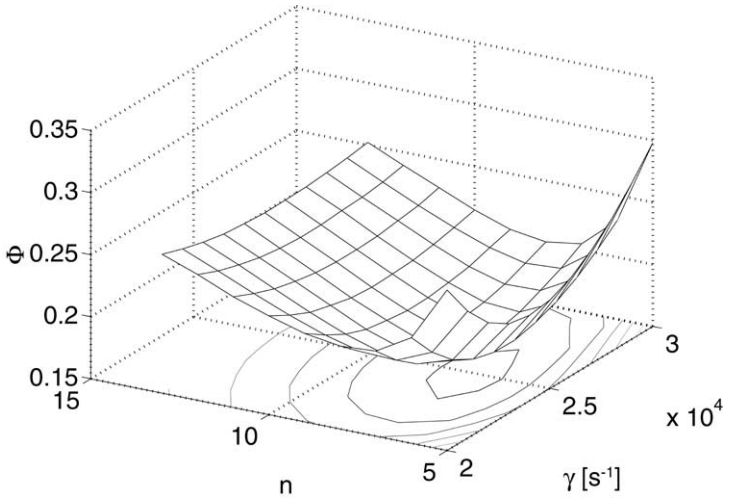

Fig. 7. The objective function, Φ, in the neighbourhood of the determined minimum.

starting parameters. These were chosen in a wide range from 0.1 to 10 times the estimated parameter values. In Fig. 7 the objective function, Φ, according to Eqs. (2) and (3) is plotted as a 3D-surface with its corresponding level curves. It is observed that, at least in the area covered by the diagram, the objective function appears to have a single minimum.

The sensitivity analysis shows substantial changes in the optimal parameter values when uncertainties of up to 5% are introduced for the measured quantities, $F^{\exp}(t)$ and $U(t)$. Fig. 8 illustrates the relative changes of the evaluated optimal parameters as functions of systematic relative errors in measured quantities. It is observed that γ is more sensitive than n to systematic errors and that γ is more sensitive to errors in $F^{\exp}$ than it is to errors in U. These sensitivities indicate that accuracy in measured quantities is highly important for the reliability of estimated material parameters.

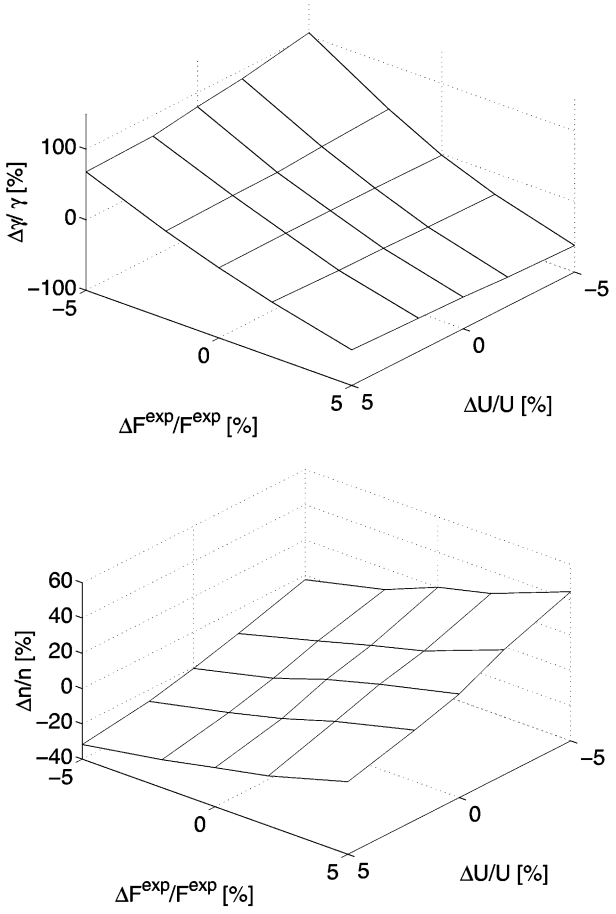

Fig. 8. Relative changes of the optimal parameters, γ and n, when uncertainties are introduced for the measured quantities $F^{\exp}(t)$ and $U(t)$.

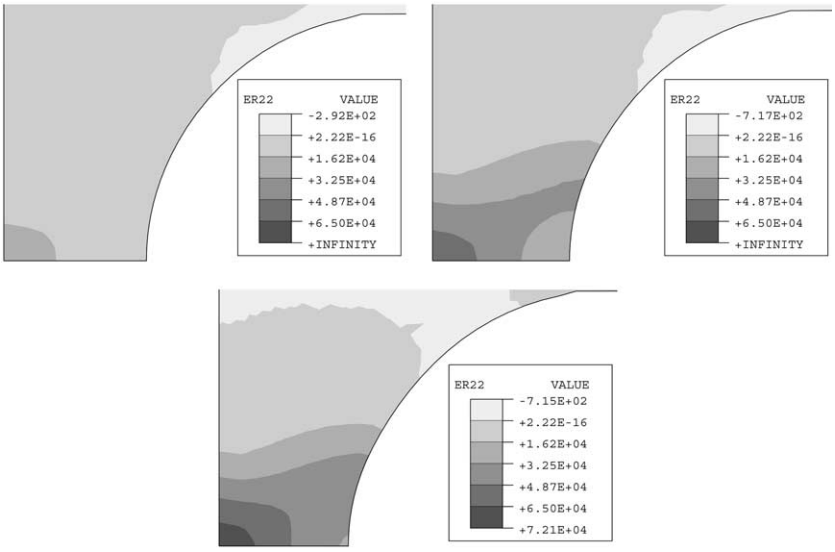

Fig. 9. Strain-rate distributions at three different instants (9.6, 10.8, 12.0 μs) during the deformation process. The instants are marked with stars in Fig. 5.

An interesting quantity to estimate is the strain rate in the ligament. In Fig. 3 where extension vs. time is plotted, the maximum extension rate can be estimated to 8 m/s for the studied time period ($t < 12$ μs). This rate divided by the ligament length, L gives a rough estimation of the strain rate of 2×10^4 s^{-1}. Another way to estimate the strain rate is to use the results from the FE-calculation with the optimum material parameters. Fig. 9 shows the distribution of the strain rate in the y-direction at three different instants (9.6, 10.8, 12.0 μs) indicated with stars in the $f^{FE}(u)$ curve in Fig. 5. These fields show that the highest strain rate is obtained in the middle of the ligament and it reaches about 7×10^4 s^{-1} at the third and latest instant. This strain rate is about three times higher than the rough estimation and this is expected for the nonhomogeneous strain field caused by the ligament geometry.

5. Conclusions

The presented method is aimed as a tool for determination of constitutive parameters under high strain-rate conditions and the basis for the method is iterative numerical simulation of experimental results or so called inverse modelling. These preliminary results indicate that the mechanical behaviour of a small specimen can be observed and evaluated at strain rates up to 10^4–10^5 s^{-1}.

A series of high-speed photographs was taken of the small ligament area during the deformation process. The quality of the frames is sufficient for investigation of the deformation and fracture process and evaluated data can be used in inverse

modelling. However, only one deformation quantity is measured in this preliminary study making results vulnerable to experimental errors.

Material parameters in Perzyna's viscoplastic model were estimated through inverse modelling and a sensitivity analysis was performed, that quantifies the relation between accuracy in evaluated parameters and in measured data. Simulation of the experiment using estimated optimal parameters showed good agreement with experimental result.

We conclude the following:

- The experimental method is promising but needs some improvement regarding resolution in the optical measurement.
- Numerical simulation of experiments is necessary and methods like Subplex facilitates the extraction of constitutive parameters.
- Microscopic high-speed photography is a powerful method to study a transient deformation process in a small specimen and with optical methods like Moiré and speckle methods more information regarding the deformation field could be recorded.

Acknowledgements

The authors are grateful to Dr. Bengt Wikman and Dr. Greger Bergman for their valuable guidance with the implementation of the Subplex algorithm. The ULTRANAC camera purchase was possible due to a grant from the Swedish Council for Planning and Coordination of Research (FRN).

References

Barlat, F., Glazov, M.V., Brem, J.C., Lege, D.J., 2002. A simple model for dislocation behavior, strain and strain rate hardening evolution in deforming aluminium alloys. Int. J. Plasticity 18, 919–939.

Blazynski, T.Z., 1987. Materials at High Strain Rates. Elsevier.

Brickstad, B., 1983. A viscoplastic analysis of rapid crack propagation experiments in steel. Journal of the Mechanics and Physics of Solids 31, 307–327.

Field, J.E., Walley, S.M., Bourne, N.K., Huntley, J.M., 1994. Experimental methods at high rates of strain. J. Phys. IV France DYMAT 94, Oxford.

Freund, L.B., Hutchinson, J., 1985. High strain rate crack growth in rate-dependent plastic solids. Journal of the Mechanics and Physics of Solids 33, 169–191.

Gilat, A., Cheng, C.S., 2000. Torsional split Hopkinson bar tests at strain rates above 10^4 s^{-1}. Experimental Mechanics 40, 54–59.

Gilat, A., Cheng, C.S., 2002. Modeling torsional split Hopkinson bar tests at strain rates above 10,000 s^{-1}. Int. J. Plasticity 18, 787–799.

Gorham, D.A., Pope, P.H., Field, J.E., 1992. An improved method for compressive stress–strain measurements at very high strain rates. Proc. R. Soc. Lond. A 438, 153–170.

Gray III, G.T., 2000. Classic split-Hopkinson pressure bar testing. ASTM Handbook: Mechanical Testing and Evaluation 8, 462–476.

Hogland, R.G., Rosenfield, A.R., Hahn, G.T., 1972. Mechanisms of fast fracture and arrest in steel. Metallurgical Transactions 3, 123–136.

Johnson, G.R., Cook, W.H., 1983. A constitutive model and data for metals subjected to large strain rates and high temperatures. In: Proc. 7th Int. Symp. on Ballistics, The Netherlands, pp. 541–547.

Johnson, G.R., Cook, W.H., 1985. Fracture characteristics of three metals subjected to various strains, strain rates, temperatures and pressures. Eng. Fract. Mech. 21, 123–136.

Khan, A.S., Liang, R., 1999. Behaviors of three BCC metal over a wide range of strain rates and temperatures: experiments and modeling. Int. J. Plasticity 15, 1089–1109.

Khan, A.S., Lopez-Pamies, O., 2002. Time and temperature dependent response and relaxation of soft polymer. Int. J. Plasticity 18, 1359–1372.

Lemaitre, J., Chaboche, J.L., 1990. Mechanics of Solid Materials. Cambridge University Press.

Liang, R., Khan, A.S., 1999. A critical review of experimental results and constitutive models for BCC and FCC metals over a wide range of strain rates and temperatures. Int. J. Plasticity 15, 963–980.

Lindholm, U.S., 1971. High strain rate tests. Measurements of Mechanical Properties. V Part 1, pp. 199–271.

Lo, K.K., 1983. Dynamic crack tip fields in rate sensitive solids. Journal of the Mechanics and Physics of Solids 31, 287–305.

Meyers, M.A., 1994. Dynamic Behaviour of Materials. John Wiley & Sons.

Muskhelishvili, N.I., 1953. Some Basic Problems of the Mathematical Theory of Elasticity. Noordhoff, Gronongen, Holland.

Nemat-Nasser, S., Kapoor, R., 2001. Deformation behavior of tantalum and a tantalum tungsten alloy. Int. J. Plasticity 17, 1351–1366.

Nilsson, P., Ståhle, P., Sundin, K.G., 1998. On the behaviour of crack surface ligaments. Nuclear Engineering and Design 184, 145–153.

Perzyna, P., 1963. The constitutive equations for rate-sensitive plastic materials. Q. Appl. Math. 20, 321–332.

Pope, P.H., Field, J.E., 1984. Determination of strain in dynamic compression test. J. Phys. Engng. Sci. Instrum. 17, 817–820.

Rowan, T.H., 1990. Functional Stability Analysis of Numerical Algorithms. PhD thesis, The University of Texas at Austin, USA.

Widehammar, S., 2002. A Method for Dispersive Split Hopkinson Pressure Bar Analysis Applied to High Strain Rate Testing of Spruce Wood. PhD thesis, ISBN 91-554-5461-5, Uppsala University, Sweden.

Zerilli, F.J., Armstrong, R.W., 1987. Dislocation-mechanics-based constitutive relations for material dynamics calculations. Journal of Applied Physics 61, 1816–1825.